Structural verification of an oil-cutting tank affected by corrosion and differential settlements

Cindy G. Wozniuk[1], Rossana C. Jaca[1], Mónica Zalazar[2], Eduardo M. Sosa[3]

[1]*Departamento de Ingeniería Civil, Facultad de Ingeniería, Universidad Nacional del Comahue*
Buenos Aires 1400, 8300 Neuquén, Argentina
geraldwoz@gmail.com, rossana.jaca@fain.uncoma.edu.ar

[2]*Departamento de Mecánica Aplicada, Facultad de Ingeniería, Universidad Nacional del Comahue,*
Buenos Aires 1400, 8300 Neuquén, Argentina
zalazar_monica@yahoo.com.ar

[3]*Department of Mechanical and Aerospace Engineering, West Virginia University,*
1306 Evansdale Drive, Morgantown, WV, 26506, United States
eduardo.sosa@mail.wvu.edu

Abstract. Crude oil cutter tanks are essential components in the hydrocarbon production process. In Argentina's Patagonia region, these metal tanks sit over a concrete platform, which may be affected by differential settlements caused by uneven compaction of the soil or damage by unexpected water flow. Additional damage can occur due to corrosion originated by the emulsifying mixture stored in the tank. This work analyzes the structural behavior of an oil cutter steel tank with evidence of damage due to localized corrosion and differential settlements and its structural response under wind loads. The analysis is implemented by modeling the tank with a multipurpose finite element code following three scenarios: tank without damage, tank damaged by corrosion measured by thickness reduction and unevenness obtained by surveying work, and progress of deterioration. Simulation results are compared with measurements carried out on a real tank using non-destructive tests. Results show that the equilibrium paths are non-linear, with clear signs of instability. The presence of imperfections, such as reduced thicknesses and vertical settlements, diverts the structure from the undamaged configuration and bifurcation buckling for much lower load levels. Reduced wall thicknesses and differential settlements generate stress concentrations that increase the deterioration of the structure.

Keywords: buckling, corrosion, settlement, tank, wind.

1 Introduction

Crude oil cutter metal tanks are essential components in the production process of the hydrocarbon industry. They carry out the water/oil separation process using chemical emulsion. The environmental impact of an oil leak or seep, even in small amounts, can have significant adverse effects on public and private property, as well as the increased potential of fire and explosion hazards. Corrosion can cause leaks, and inadequate control poses serious environmental and safety hazards (Thakur [1]). During its operational years, tanks can also be affected by uniform or differential settlement of the base, caused by lack of or improper compaction of the surrounding supporting soil or improper rainwater runoff. The settlements in the support base generate significant deformations in the cylindrical shell, and corrosion generates a progressive decrease in its thickness. Different authors have reported the influence on buckling loads due to the presence of geometric imperfections (Hornung and Saal [2], Paor et al. [3], Jaca et al. [4]).

Different types of corrosion can affect tanks. In microbiological corrosion, sulfate-reducing bacteria accelerates the speed of the process by increasing the formation of sulfuric acid. Underground corrosion is typical of tank settlements, and it is related to the deterioration of metals exposed to wet or corrosive soils. Damage occurs mainly by thickness reduction on the metal, and poor coating conditions exacerbate it. In this regard, Lu et al. [5] analyzed the factors that influence corrosion processes considering the chemical components of the fluid. Jei et al. [6] investigated improvements in the corrosion resistance of steel.

Settlements of the tank base can be uniform or differential and typically generate a loss of circularity in the upper portions of the tank, which in turn produces additional stresses. This problem has been studied by Jonaidi et al. [7], who reported the structural consequences of differential settlements in axil-symmetric shells. Similarly, Godoy and Sosa [8] analyzed the effect of localized settlements on storage tanks, and Gong et al. [9] and [10], Cao and Zhao [11], and Zhao et al. [12] conducted studies to evaluate the buckling of shells produced by settlement in some sectors of the tank foundation.

This work presents the results of the evaluation of the in-service condition of a tank with corrosion damage and differential settlements based on the results of periodic regulatory inspections (API 653 [13], API 580 [14]), and the verification of its response under wind loads. The research is based on external visual inspection tests, ultrasound, and topographic surveys where the thicknesses were measured at different points of interest.

2 Materials and Methods

The tank considered for this study is a 34-m-diameter (D), 12-m-high shell (H) with a liquid level design height of 11.4 m, and a 4-m-high self-supporting umbrella-type roof (Fig. 1(a)). The tank material is ASTM A36 steel with a modulus of elasticity of E = 206 MPa and a Poisson's ratio of ν = 0.3. The thickness of the roof is 0.015 m, the cylindrical shell has variable thicknesses calculated by the method of 1 foot (API 650 [15]) and their values are presented in Tab. 1. Figure 1(b) shows the geometric model created for this research.

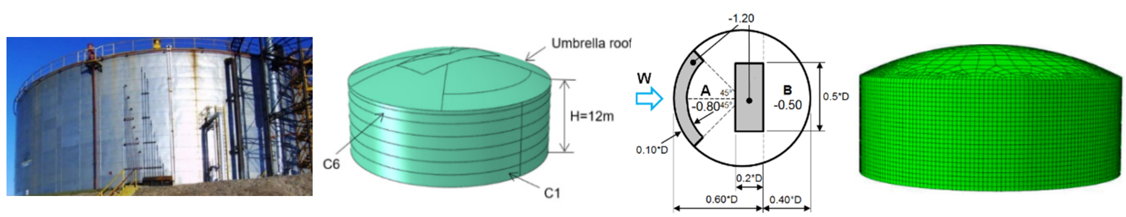

(a) (b) (c) (d)

Figure 1. (a) Reference tank, (b) Geometric model of the tank and shell courses, (c) Pressure coefficients over tank's roof, (d) Finite element model

Table 1. Thickness of shell courses

Courses	C1	C2	C3	C4	C5	C6
Thickness [m]	0.0136	0.0115	0.0094	0.0073	0.006	0.006

The tank is located in the Argentinian Patagonia, where high wind speeds are frequent. Snow and seismic loads are negligible compared to the magnitude wind loads and are not considered in this work. The wind pressure (q_z in N/m^2) was evaluated according to eq. (1) (CIRSOC 102 [16]), where the basic wind speed V at the installation area is 62 m/s (223 km/h), the exposure coefficient for constant dynamic pressure is K_z = 1.05, the topography factor is K_{zt} = 1, the wind directionality factor is K_d = 0.95, and the importance factor is I = 1.15. The wind pressures around the cylindrical shell followed a circumferential distribution. C_p's external pressure coefficients were calculated as a function of the angle ϕ measured from the windward meridian and defined by eq. (2). Figure 1(c) shows the variation of C_p in the different partitions created on the tank roof.

$$q_z = 0.613\, K_z\, K_{zt}\, K_d\, V^2 I. \tag{1}$$

$$C_p(\phi) = -0.5 + 0.4\,cos(\phi) + 0.8\,cos(2\phi) + 0.3\,cos(3\phi) - 0.1\,cos(4\phi) - 0.05cos(5\phi). \tag{2}$$

Simulation models were created using a general-purpose finite element simulation package (Abaqus [17]). The cylindrical shell and the roof were discretized with quadratic and reduced integration shell elements (S8R5) (Fig. 1(d)). The typical element size for the cylindrical shell was 0.5 m (convergence with a relative error of 0.3%) and 1.3 m for the roof. The cylindrical shell sits on a concrete ring, represented by boundary conditions of restricted nodal displacements but allowing nodal rotations.

The tank was modeled considering its original configuration and its deformed configuration to obtain the structural behavior differences. The tank response was analyzed at three stages of its operational life, including a) Initial state: without corrosion damage or differential settlements, b) Current state: considering the measured corrosion and differential settlements evaluated in the measurements on the deformed tank, and c) Future state: representing the advance of corrosion and differential settlements. Corrosion was represented by reducing the thickness of the elements at the regions affected by corrosion, and the magnitude of localized settlements was obtained from field measurements.

Three types of analysis were carried out in this study: Linear Bifurcation Analysis (LBA), Geometric Nonlinear Analysis (GNLA), and Geometric Nonlinear Analysis with Imperfections (GNIA) implemented using the Riks algorithm [18]. LBA produced eigenvalues and eigenvectors that allowed obtaining critical loads and associated critical modes used as a first approximation to calculate the values in which equilibrium instability problems appeared. The geometric imperfections corresponded to the reduction of thickness due to corrosion and differential settlements. The influence of corrosion and foundation settlements for the hydrostatic pressure of the fluid was studied separately and later combined to obtain the behavior under the action of the wind.

3 Simulation cases and results

3.1 Influence of the reduction of thickness due to corrosion

The region of the tank close to the foundation ring was the most affected by corrosion. The reduction in thickness was evaluated using an ultrasound technique in which several measurements were taken over the perimeter along a 14-m wide and 1-m high strip (Fig. 2). Given that the thicknesses vary, measurements were grouped in sectors of similar thickness, resulting in 4 groups called Group 1 to 4 with thicknesses of 9.24 mm, 4.09 mm, 4.01 mm, and 1.91 mm, respectively shown in Fig. 2. The zone affected by corrosion coincides with the tank's windward portion and constitutes one of the most unfavorable loading situations.

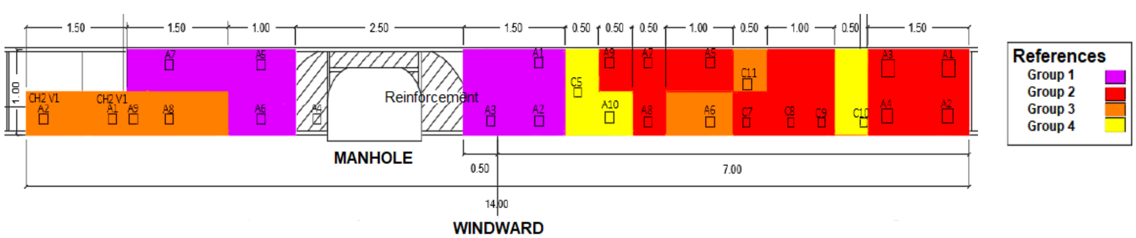

Figure 2. Thickness groups in the tank shell

If no corrosion is present, the most unfavorable condition for buckling of the tank shell corresponds to an empty tank under wind pressure. For this condition, the critical load determined by LBA was λ_c = 1.95 kPa, and buckling occurred in the upper half of the windward envelope, as shown in Fig. 3(a). From the critical load and eq. (1) it was possible to back-calculate an actual wind speed of 52.6 m/s, which is 15% lower than the 62 m/s required by the regulations and location of the tank.

When the tank was modeled considering its current state, i.e., affected by corrosion, the critical load decreased slightly (λ_c =1.94 kPa). The buckling shape was similar to the case without corrosion. However, when the tank was modeled considering a future state in which the effects of corrosion gradually reduced the thicknesses, there was a change in the buckling shape, as shown in Fig. 3(b). In this case, buckling occurred in the area of reduced thickness with a critical load of λ_c = 1.85 kPa (V = 51.3 m/s). Additional simulations indicated that if the thicknesses continued being reduced, the buckling shape was maintained, but the critical load reduced until reaching an associated velocity of V = 10.9 m/s. Simulation results also showed that the advancement of corrosion around the entire perimeter in the future state did not substantially modify the response compared to considering only windward corrosion.

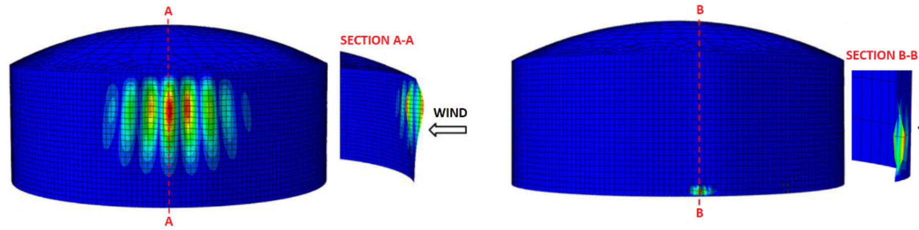

(a) (b)

Figure 3. Critical mode under wind: (a) No corrosion (λ_c=1.95 kPa), (b) Propagated corrosion (λ_c=1.85 kPa)

3.2 Influence of differential settlements at the base

The measured support settlements were grouped into two areas. The displacements increased following an approximately linear pattern combined with a region where the displacements followed a constant amplitude with a maximum measured displacement of 0.1 m, as illustrated in Fig. 4. The portion of the cylindrical shell affected by the support settlement had an arc length of 16 meters. LBA indicated that the critical load of the first buckling mode was λ_c = 0.232; that is, buckling occurred at approximately 23% of the maximum measured displacement (0.02 m). This value is of the order of magnitude of the thickness of the shell in the buckled area. The critical buckling mode for the measured settlements is shown in Fig. 4, where it can be seen that the vertical settlements produced dents coinciding with the portion of the tank where the settlements with the greatest linear variation are found.

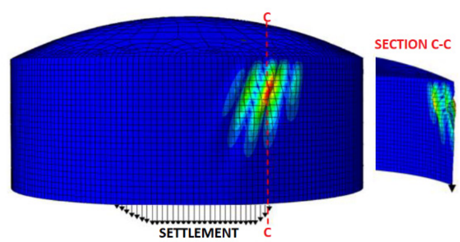

Figure 4. Critical buckling mode with measured support settlements (λ_c = 0.232)

A GNLA was performed to obtain the deflected shape of the tank when subjected to base displacements reduced to half their measured value. Figure 5(a) shows the deformation of the tank obtained from the GNL simulation. The buckled shape shows elliptical dents located in the upper region of the cylindrical shell with the most significant out-of-plane displacements near the region of the highest settlement gradient.

Figure 5(b) shows the equilibrium path of the node with the greatest out-of-plane displacement (Node A). The out-of-plane displacement increases with the vertical descent, for a settlement value of 0.0025 m, where the fundamental path intersects with another post- critical (secondary) equilibrium path that may not be present at the origin of the loading process. The displacements of the base are reversed, and the displacement of Node A increased indefinitely, resulting in an unstable equilibrium.

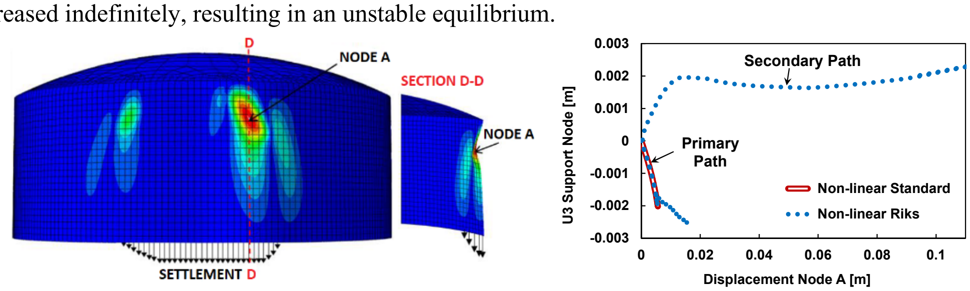

(a) (b)

Figure 5. Vertical settlements: (a) Deformed shape, (b) Equilibrium path for node A corresponding to highest out-of-plane displacement

3.3 Combined effects of wind and vertical settlements

A particularly unfavorable loading condition corresponds to the presence of support settlements at the windward location of the tank. This case was analyzed through an LBA, which predicted a similar critical mode like the one shown in Fig. 4, and also a critical buckling load of $\lambda_c = 0.23$ kPa, which was obtained from imposing a maximum support displacement of 0.020 m, and before the activation of the wind load. The action of the wind was considered in a GNLA, and the resulting deformed shape is shown in Fig. 6(a). The dents of the buckled shape were not located on the meridians that underwent the highest vertical descent and displayed an oblique shape. The equilibrium path of Node B illustrated in Fig. 6(b) shows that as load increased, the displacement at Node B also increased. When the displacement reached a value of 0.018 m (λ_{max}= 0.2), the system adopted a secondary non-linear path that intersected the fundamental path at the bifurcation point.

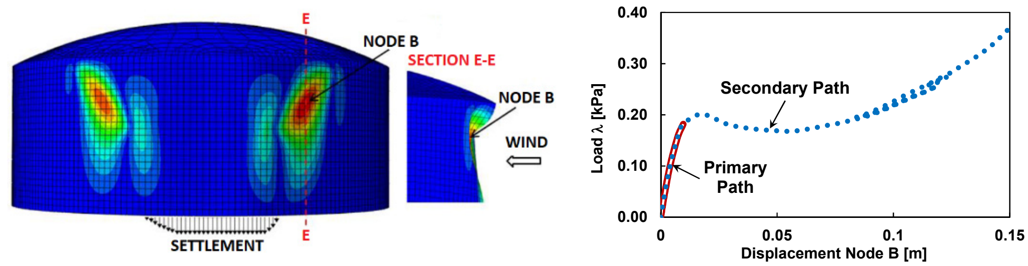

(a) (b)

Figure 6. Wind and vertical settlements (a) Deformed shape, (b) Equilibrium path for Node B (highest out-of-plane displacement)

3.4 Analysis of the tank in the current state

An LBA was used to evaluate the tank with corrosion and measured support settlements without considering the wind load. This analysis allowed calculating the critical buckling mode (Fig. 7) and its associated critical load ($\lambda_c = 0.093$). Results show that the buckling dents occurred at the lower shell course at the area's location with reduced thickness, slightly shifting from the meridians with the highest vertical settlements. For a maximum settlement amplitude of 0.05 m, buckling occurred at only about 9% of this value, which corresponds to the vertical displacement of 0.005 m. This value is much lower than the maximum measured settlement and is in the order of the thickness reduced by corrosion. A GNIA analysis showed that the response of the structure is similar to that obtained for the case in which there are only differential settlements of the base (Node A in Fig. 5(a)).

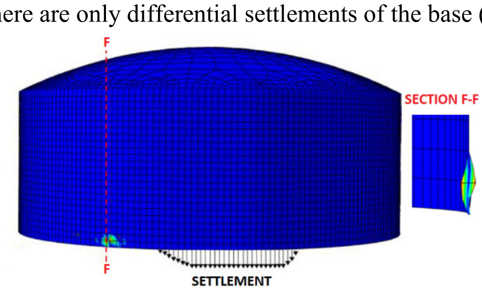

Figure 7. Critical mode with corrosion and measured settlements ($\lambda_c = 0.093$)

When considering the wind stress in the LBA analysis, the critical load and mode for which the buckling occurs coincided with the one shown in Fig. 7 (current settlements and corrosion without wind). When evaluating the post-critical behavior using GNIA, the response was similar to the one shown in Fig. 6. The system adopted a secondary path for $\lambda = 0.2$ kPa, and subsequent displacements increased indefinitely and resulted in an unstable equilibrium path.

3.5 Analysis of the tank in a future state.

The future structural behavior of the tank was modeled considering a combination of differential settlements, with a shell having the minimum thickness measured upwind and adopted for all corrosion groups (1.91 mm) and subjected to wind pressure. The zone affected by corrosion is considered to be located windward as it would be a more unfavorable situation. Figure 8 shows the critical buckling mode corresponding to a critical load $\lambda_c = 0.035$, which indicates that buckling occurs at about 3% of the maximum settlement. The instability occurs for approximately 1.7 mm of vertical displacement, which is a value in the order of the minimum thickness measured. The buckling dents are located at regions with reduced thickness due to corrosion, and their location does not coincide with the area where the maximum vertical settlement occurs.

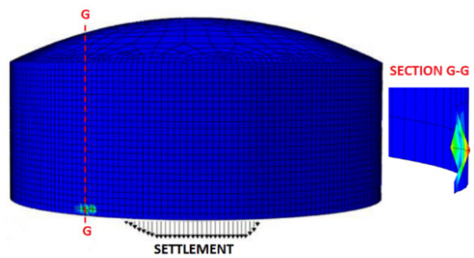

Figure 8. Critical buckling mode with settlements and minimum thickness measured ($\lambda_c = 0.035$)

The deflected shape obtained from a GNIA that included the wind effects is illustrated in Fig. 9 (a). In this deformed shape, the node with the highest out-of-plane displacement (Node C) followed a nearly linear path up to a displacement of 0.001 m. It then adopted a secondary path with $\lambda = 0.03$ kPa and followed by an increasing non-linear behavior. The displacements are an order of magnitude lower than the thickness of the shell course.

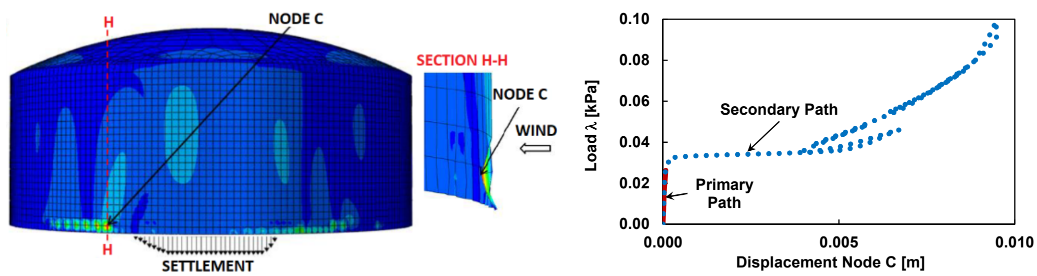

(a) (b)

Figure 9. Future state of the tank: (a) Deformed shape, (b) Equilibrium path (Node C)

4 Discussion

The analysis results show that the variation in the response is negligible if the corrosion extends over the entire perimeter of the tank or is only located windward. The critical wind loads obtained with reduced shell thicknesses decreased and resulted lower than the values required by the regulations (CIRSOC 102 for 62 m/s). The buckling modes showed nearly elliptical shapes with a nearly vertical orientation in the windward zone with out-of-plane displacements resulted in one order of magnitude greater than the thickness of the cylindrical shell.

For a small range of vertical settlement values (in the order of shell thickness), results showed that equilibrium paths exhibited a linear behavior. As the amplitude of the settlement increased, the maximum out-of-plane displacements moved significantly away from the linear solution, adopting a secondary path. Results showed that for 20% of the measured maximum settlement value, the structure is already in a post-critical state with unstable equilibrium, in which displacements can increase indefinitely and potentially lead to a future collapse.

When the structure is subjected to wind loads, the buckling dents coincide with meridians subjected to vertical settlement. When the tank is subjected to differential settlements followed by wind loads, combined or not with the effects of corrosion, results indicate that equilibrium instability occurs before the wind loading suggesting that the effects of the differential settlements mainly influence the structural response.

5 Conclusion

A series of simulations were carried out to analyze the structural behavior of an oil-cutting tank affected by corrosion, differential settlements, and wind loads. Results indicate that if the corrosion is only upwind, the behavior is more unfavorable than covering the entire perimeter. In all the modeled cases, buckling occurs for wind speeds lower than the regulatory speed in the area where the tank is located. The measured settlement pattern generates elliptical and inclined dents, possibly due to asymmetric settlements that coincide with the settled meridians. When the wind is added to the vertical settlement, the deformed area moves towards the sector without base displacements and tends to increase permanently.

When the tank is analyzed for service conditions, the combination of corrosion, support settlements, and wind pressure produces an unstable behavior for wind speeds lower than values required by the regulations. In a possible scenario of corrosion propagation with a reduction in thickness, the most significant out-of-plane displacements could occur in the area close to the supports and outside the sector with settlements at notably lower wind speeds.

Acknowledgments. The authors are grateful for the support provided for this work by the SECYT-UNCo.

Authorship statement. The authors hereby confirm that they are the solely liable persons responsible for the authorship of this work, and that all material that has been herein included as part of the present paper is either the property (and authorship) of the authors or has the permission of the owners to be included here.

References

[1] A. K. Thakur, "Corrosion Control for Above Ground Crude Oil Storage Tanks". *Corrosion 2017*, New Orleans, USA, 2017.
[2] U.Hornung and H Saal, "Buckling loads of tank shells with imperfections". *International Journal of Non-Linear Mechanics*, vol. 37, n.4-5, pp. 605-621, 2002.
[3] C. de Paor, K. Cronin, J. P. Gleeson, and D. Kelliher, "Statistical characterisation and modelling of random geometric imperfections in cylindrical shells". *Thin-Walled Structures*, vol. 58, pp.9-17, 2012.
[4] R. C. Jaca, L. A. Godoy, F. G. Flores, and J. G. Croll, "A reduced stiffness approach for the buckling of open cylindrical tanks under wind loads". *Thin-Walled Structures*, vol. 45, pp. 727-736, 2007.
[5] Y. Lu, Z. Wang, Z. Dou, Y. Zhen, and F. Jiang, "Study of corrosion of oil tank parts and gas-phase space in different tanks", *Process Safety Progress*, vol. 37, n.3, pp. 419–426, 2018.
[6] W. Jie, Z. Yangtao, D. Junhua, H. Xiaoyan, and K. Wei, "Effect of cementite spheroidization on improving corrosion resistance of pearlitic steel under simulated bottom plate environment of cargo oil tank." *Materialia*, vol.6, 2019.
[7] M. Jonaidi and P. Ansourian, "Harmonic settlement effects on uniform and tapered tan shells". *Thin-Walled Structures*, vol.31, n.1-3, pp. 237-255, 1998.
[8] L.A.Godoy y E.M. Sosa, "Localized support settlements of thin-walled storage tanks". *Thin-Walled Structures*, vol.41, pp. 941-955, 2003.
[9] J. Gong, W. Cui and S. Zeng, "Buckling analysis of large scale oil tanks with a conical roof subjected to harmonic settlement". *Thin-Walled Structures,* vol.52, n.7, pp. 143-148, 2012.
[10] J. Gong, J. Tao, J. Zhao, S. Zeng, and T. Jin, "Buckling analysis of open top tanks subjected to harmonic settlement". *Thin-Walled Structures*, vol.63, pp.37-43, 2013
[11] Q. S. Cao and Y. Zhao, "Buckling strength of cylindrical steel tanks under harmonic settlement". *Thin-Walled Structures*, vol. 48, n. 6, pp. 391-400, 2010.
[12] Y. Zhao, Q. S. Cao, and W. Y. Xie, "Floating roof steel tanks under harmonic settlement: FE parametric study and design criterion". *Journal of Zhejiang University, Science A*, vol.7, n. 3, pp.398-406, 2006.
[13] API 653. *Tank Inspection, Repair, Alteration and Reconstruction*, American Petroleum Institute, Washington, DC, 2013.
[14] API 580. *Risk-Based Inspection*, American Petroleum Institute, Washington, DC, 2016.
[15] API 650.*Welded steel tanks for oil storage*, American Petroleum Institute, Washington, D.C., 2010.
[16] CIRSOC 102, Acción del viento sobre las construcciones. Centro de Investigación de los Reglamentos Nacionales de Seguridad para Obras Civiles. Buenos Aires, (2005).
[17] ABAQUS. *User's Manuals*, Version 6.3. Hibbitt, Karlsson and Sorensen, Rhode Island, 2006.
[18] E. Riks, "An incremental approach to the solution of snapping and buckling problems", *Int. J. Solids Struct*., vol. 15, pp.529-551, 1979.